

# Formation of exotic baryon clusters in ultra-relativistic heavy-ion collisions.

A.S. Botvina<sup>1,2</sup>, J. Steinheimer<sup>1</sup>, M. Bleicher<sup>1,3</sup>

<sup>1</sup>*Frankfurt Institute for Advanced Studies and ITP J.W. Goethe University,*

*D-60438 Frankfurt am Main, Germany*

<sup>2</sup>*Institute for Nuclear Research, Russian Academy of Sciences, 117312 Moscow, Russia and*

<sup>3</sup>*John von Neumann Institut für Computing (NIC),*

*Jülich Supercomputing Centre, FZ Jülich, D-52425 Jülich, Germany*

(Dated: March 13, 2018)

## Abstract

Recent experiments at RHIC and LHC have demonstrated that there are excellent opportunities to produce light baryonic clusters of exotic matter (strange and anti-matter) in ultra-relativistic ion collisions. Within the hybrid-transport model UrQMD we show that the coalescence mechanism can naturally explain the production of these clusters in the ALICE experiment at LHC. As a consequence of this mechanism we predict the rapidity domains where the yields of such clusters are much larger than the observed one at midrapidity. This new phenomenon can lead to unique methods for producing exotic nuclei.

PACS numbers: 25.75.-q , 25.75.Dw , 25.75.Ld , 21.80.+a

## I. INTRODUCTION

In relativistic nuclear collisions an abundance of new particles consisting of all kind of quark and anti-quark flavors is produced. During the late stage of the collision these particles can interact in secondary processes and produce novel clusters containing several baryons. In this case, promising studies of fragmentation reactions probing the limits in isospin space of light nuclei, exotic nuclear states, anti-nuclei, and multiple strange nuclei are feasible. Recently very encouraging results on the formation of exotic clusters come from experiments at relativistic colliders: For example, STAR at RHIC [1, 2], and ALICE at LHC [3, 4] have observed hyper-tritons and anti-hyper-tritons. Experimental programs to search for more heavy exotic nuclear species are now underway [5, 6]. Therefore, a theoretical understanding of these phenomena is necessary. Transport models have been used to successfully describe many observables, including strangeness production at intermediate energies [7–11]. At very high energy most of the state-of-art hybrid models apply a hydro-dynamical expansion of the hot and dense matter and a subsequent microscopic transport approach to describe the hadronic rescattering (see, e.g., for UrQMD, Ref. [12, 13]). In the framework of microscopic transport models a coalescence prescription for the formation of the composite clusters can be naturally applied [14–17]. In this paper we demonstrate the effectiveness of the transport-plus-coalescence approach for the description of data at LHC energies. Important predictions for the future research of baryon clusters in the ultra-relativistic heavy-ion collisions are also presented.

## II. MODELS FOR PRODUCTION OF LIGHT CLUSTERS AT RELATIVISTIC COLLISIONS

Thermal and coalescent mechanisms to produce complex nuclei in high energy collisions have been discussed in previous works (see, e.g., [18, 19]). The thermal models allow for a good description of the particle production yields, for example, in the most central collisions [20, 21]. For this reason we believe that the produced particles do widely populate the available reaction phase space, and this should be taken into account in any interpretation of the data. Only the lightest clusters, with mass numbers  $A \lesssim 3-4$ , can be noticeably produced in this case because of the very high temperature of the fireball ( $T \approx 160$  MeV).

However, the pure thermal models can not describe the energy spectra of particles and their flows. Also in non-central collisions the dynamics and secondary interactions in the projectile and target residues will influence the nucleon clusters (fragments) production. As was shown, the thermal and coalescence descriptions are naturally connected: In particular, there is a relation between the coalescent parameter, density, temperature, and binding energies of the produced clusters [22]. In the following we consider the dynamical transport and coalescence mechanisms, because they have predictive power for many observables. There were also numerous discussions that even in central collisions of very high energy the coalescence mechanism, which assembles light fragments from the produced hyperons and nucleons (including anti-baryons), may be essential [1, 2].

The first reaction step should be the dynamical production of baryons which later on can be accumulated into clusters. The transport model Ultrarelativistic Quantum Molecular Dynamics (UrQMD) is quite successful in the description of a large body of data. In the standard formulation [9, 10] the model involves string formation and its fragmentation according to the PYTHIA model for individual hard hadron collisions. The current versions of UrQMD include up to 70 baryonic species (including their anti-particles), as well as up to 40 different mesonic species, which participate in binary interactions. This work is focused on very high energies and we employ the UrQMD transport model [23] in the hybrid mode for the description of the dynamical evolution in central collisions. In this mode the propagation is composed of an ideal 3+1d fluid dynamical description for the dense phase, which is mainly comprised of a strongly interacting quark gluon plasma (QGP). The event-by-event initial state for the fluid dynamical evolution is calculated using the PYTHIA version implemented in the UrQMD model, where the starting time of the fluid dynamical evolution is set to  $\tau_0 = 0.5$  fm/c. The equation of state, which governs the dynamical evolution has been discussed in detail in Ref. [24] and describes the transition from a hadronic system to the QGP as a smooth crossover at low baryon densities. Once the system dilutes, and the fluid dynamical description is no longer valid, the propagated fields are transformed into particles via a sampling of the Cooper-Frye equation [25]. Here we explicitly conserve the net-baryon number, net-electric-charge, and net-strangeness as well as the total energy and momentum. After this transition all hadrons continue their evolution and may interact via the hadronic cascade part of the UrQMD model. This dynamical decoupling takes on the order of 10–20 fm/c and has a significant influence on the observed hadron multiplicities

[26, 27] and spectra [12], which is strongest for most central collisions. Consequently it has been shown that this model reasonably describes hadron spectra observed by the ALICE collaboration [12], in particular the proton spectra which are essential for the study of nuclei production.

The advantage of the Monte-Carlo transport final state description is that it provides event-by-event simulations of the baryon production. This is important for investigating correlation phenomena. The coalescent procedure is ideal for the description of the baryon accumulation into clusters on event-by-event basis. It was shown before that the coalescence criterion, which uses the proximity of baryons in momentum and coordinate space, is very effective in description of light nucleon fragments at intermediate energies [14–16, 19]. After the dynamical stage described by the UrQMD model we apply a generalized version of the coalescence model [17] for the coalescence of baryons (CB). In such a way it is possible to form primary fragments of all sizes, from the lightest nuclei to the heavy residues, including hypernuclei and other exotics within the same mechanism. It was previously found [17] that the optimal time for applying the coalescence (as a final state interaction) is around 40–50 fm/c after the initial collisions of heavy-ions, when the rate of individual inelastic hadron interactions decreases very rapidly. A variation of the time within this interval leads to an uncertainty in the yield around 10% for a fixed coalescence parameter. This is essentially smaller than the uncertainty in the coalescence parameter itself. The most important CB parameter is the maximum variance between velocities of baryons  $v_c$  in a coalescent cluster.  $v_c$  should be around  $v_c \approx 0.1c$  for the lightest clusters, to be consistent with their binding energy. This value is also supported by a comparison to experimental data at energies around 1–10 A GeV [14]. We should note that our formulation of the coalescence model is microscopic, therefore, it takes into account all correlations and fluctuations of the particle production during the dynamical stage. For this reason we need a smaller coalescence parameter in order to describe the data than the parameters obtained in the analytical formulation of the coalescence [28]. In principle, the coalescence to clusters with  $A > 4$  is also possible, however, these heavy clusters are expected to be excited and their following decay can be described with the statistical models [29, 30]. Usually such big primary fragments can be produced only in peripheral collisions from nuclear residues in the projectile and target rapidity region [17]. The advantage of the sequential approach (dynamics + coalescence + statistical decay) is the possibility to predict the correlations

and fluctuations of the yields of all nuclei, including their sizes, with the rapidity, and with other produced particles. However, in the midrapidity region, because of a very large energy deposition, we expect the formation of small clusters only. In the following we concentrate on the LHC heavy-ion reactions, and on the latest results on light cluster production obtained by the ALICE collaboration [31–33].

### III. COMPARISON WITH EXPERIMENTAL DATA

We start with an analysis of the particle spectra as observed in the experiments. In Fig. 1 we show experimental data on transverse momentum distributions of protons, deuterons, and  $^3\text{He}$  particles measured at LHC by the ALICE group [31, 32]. The collisions of  $^{208}\text{Pb}$  on  $^{208}\text{Pb}$  have been performed at a center of mass energy of  $\sqrt{s}=2.76$  TeV per nucleon. The yields in Fig. 1 are obtained for the central events (top 20% of the maximum particle multiplicity) are normalized to the number of events. The rapidity range for detected particles was  $y=(-0.5$  to  $+0.5)$  in the center of mass system. The experimental data are given by symbols inside boxes presenting the systematical uncertainties which are usually larger than the statistical ones. The statistical error bars are given if they are larger than the symbol sizes. This data presentation provides consistent information on yields and distributions of produced particles needed for verification of our models. The UrQMD hybrid calculations (including the hydro-dynamical evolution of matter) with the following CB calculations are shown by the lines. The different line styles depict variation of the coalescence parameter  $v_c$  by 40%. It is important that it is possible to reproduce very good the spectra of protons with UrQMD, since in the coalescence approach the yields of all clusters depend crucially on the baryon distributions. We should note that the yields at very high transverse momenta  $P_T > 3 - 4$  A GeV are possibly dominated by jets, which are not currently included in the hydrodynamical evolution of the system. Therefore, we limit the fragments under study to  $P_T \lesssim 2 - 3$  GeV per nucleon.

One can see that the spectra of deuterons ( $^2\text{H}$ ) and helium-3 ( $^3\text{He}$ ) can be reasonably described with the coalescent parameters  $v_c=0.07c$  and  $v_c=0.1c$ , respectively. The larger value of  $v_c$  for  $^3\text{He}$  is consistent with the larger binding energy of  $^3\text{He}$  in comparison with  $^2\text{H}$ . We note that the effect of the  $v_c$  parameter is essentially bigger for large clusters. We could get a better agreement by tuning the coalescent parameters, however, this kind of

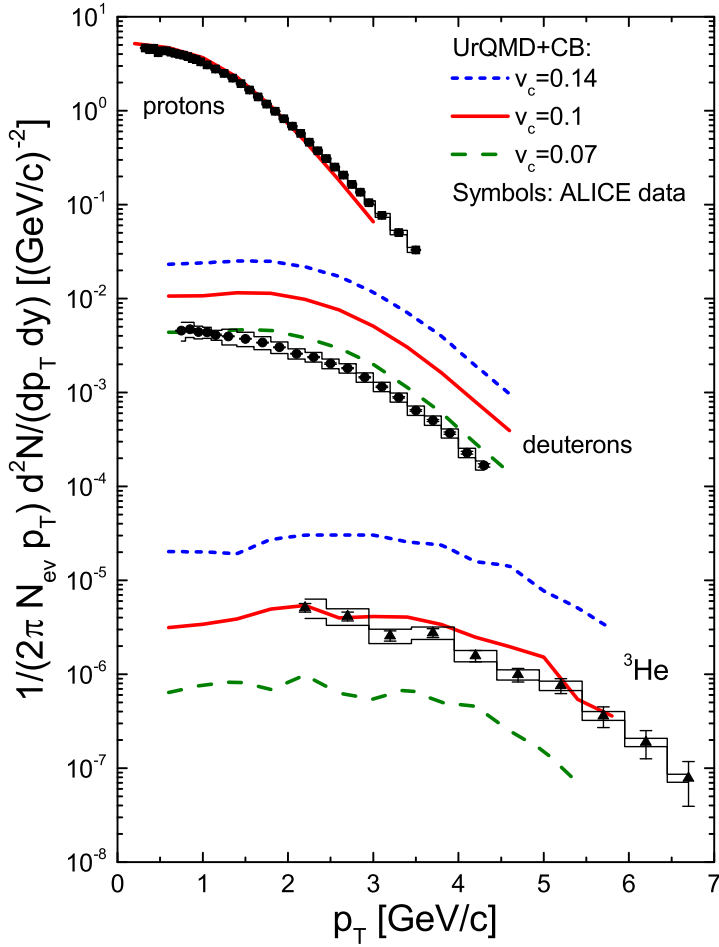


FIG. 1: (Color online) Transverse momentum spectra of protons, deuterons, and  ${}^3\text{He}$  particles in  ${}^{208}\text{Pb}$  on  ${}^{208}\text{Pb}$  collisions at the center of mass energy  $\sqrt{s}=2.76$  TeV per nucleon. The symbols with systematical (thin boxes) and statistical errors are ALICE experimental data [31, 32] in the center-of-mass rapidity range from  $-0.5$  to  $+0.5$ , and normalized per number of events for the 20% most central events. The UrQMD coupled with coalescence of baryons (CB) calculations of the same particle spectra at the same conditions are shown by short-dashed (blue), solid (red) and long-dashed (green) lines for the corresponding coalescence parameters  $v_c$  (see in the figure).

phenomenological fitting is out of our theoretical study. It is more important that the form of the distributions is independent on  $v_c$  in the wide range and corresponds to experimental distributions. This gives us a confidence to claim that the coalescence can naturally describe the production of these clusters.

Another verification of the coalescence mechanism should come from angular distributions

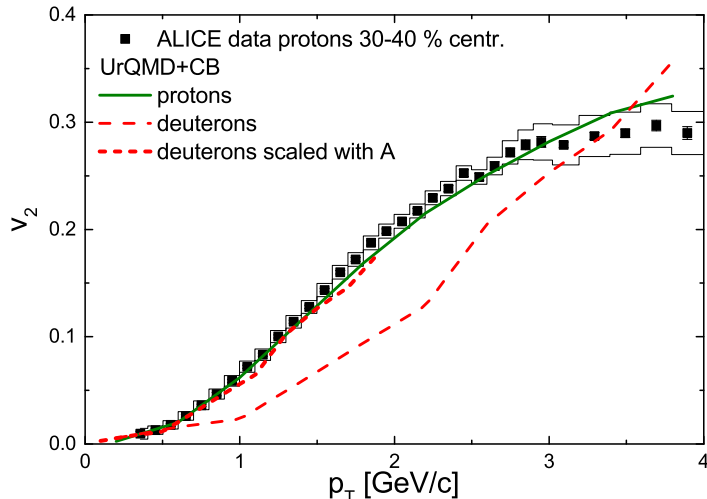


FIG. 2: (Color online) Elliptic flows ( $v_2$ ) of produced protons and deuterons versus their transverse momenta. The reactions and the rapidity range are as in Fig. 1, however, the semicentral collisions (with the centrality range of 30% – 40%) are selected. The ALICE experimental data [33] for protons are the square symbols with errors within the thin boxes. The solid (green) and long-dashed (red) lines are the UrQMD and CB calculations for protons and deuterons respectively. The short-dashed red line presents the scaled distribution for deuterons (see the text).

of the produced particles and their correlations respective to the reaction plane. We note that the angular (azimuthal) distribution of produced particles in the plane perpendicular to the beam axis is anisotropic with the corresponding maximum in the reaction plane. That is an expected consequence of the dynamical emission in such high energy collisions. A very informative observable is the elliptic flow  $v_2$ . Sometimes it is difficult to extract the reaction plane in the experiment, because of particle fluctuations in the collision events. In this case, particle correlation methods are used [33]. For the present calculations we employ the reaction plane method in each collision, and, therefore, we can find  $v_2$  for all particles by averaging their momenta perpendicular to the beam axis:  $v_2 = \langle (P_x^2 - P_y^2) / P_T^2 \rangle$ , where  $P_x$  is the momentum in the reaction plane, and  $P_T^2 = P_x^2 + P_y^2$  is the transverse momentum. The averaging is done over all events containing these particles. It was shown that the reaction plane method provides results compatible with high-order event plane (correlation) methods [34]. Therefore,  $v_2$  trends versus  $P_T$  should be a solid observable for comparison.

We present  $v_2$  measured by ALICE for protons in  $^{208}\text{Pb}$  on  $^{208}\text{Pb}$  reactions at  $\sqrt{s}=2.76$

A TeV for semi-central collisions [33] in Fig. 2. The semi-central events, which cover a centrality domain from 30% to 40% of the total particle multiplicity distribution, were used in this analysis. The UrQMD + CB calculations were performed under the same conditions for both protons and deuterons. One can see that the calculations describe the data for protons good, and they predict a rather different behaviour of  $v_2$  versus  $P_T$  for deuterons. However, our calculations lead to an interesting result: Namely, if we plot  $v_2/A$  versus  $P_T/A$  for protons ( $A=1$ ) and deuterons ( $A=2$ ), they are overlapping each other. Such a 'scaled' curve for deuterons is demonstrated by the short-dashed line in Fig. 2. This kind of 'scaling' of  $v_2$  in the coalescence mechanism can be easily explained by the averaging procedure over the produced particles: When individual nucleons have nearly the same momenta the expression  $(P_x^2 - P_y^2)/P_T^2$  does not change after their clusterizing. However, the number of nucleons is by  $A$  times larger than the number of clusters. The observation of such a coalescence scaling in experiments could be an additional verification of a pure coalescence mechanism. It is interesting that the scaling behavior has been observed in the experiments [33], however, in the elliptic flow of hadrons by taking into account the number of the constituent quarks. The quark coalescence was also discussed theoretically [35]. We believe this effect should be much stronger in our case of light nuclei, since the nuclear binding energy is much smaller than the nucleon masses and the scaling itself depends on the coalescence parameter rather weak.

#### IV. PREDICTIONS FOR THE CLUSTER RAPIDITIES

Due to technical realization of the UrQMD hybrid model [12] we have presented coalescence results from this model in the midrapidity range of central and semi-central Pb+Pb collisions only. It is however instructive to study also the rapidity dependence of cluster production, including peripheral collisions, as the produced systems properties may change essentially with rapidity. For example, special properties of nuclear matter near the hadron fragmentation region were discussed long ago [36]. It was suggested that the hadron matter of this region would have a significant non-zero net baryon number and high density [37]. Also the transverse momentum distributions of produced particles and fragmented nucleons may be different, that can have a significant effect on nuclei formation. In order to make an estimate on the rapidity distribution of nuclear clusters at the LHC we use the standard

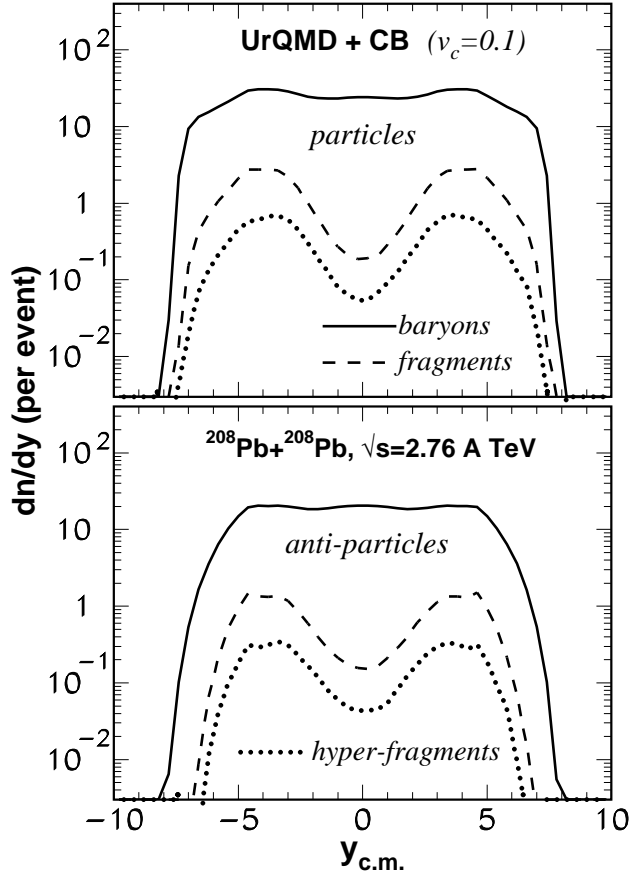


FIG. 3: The total rapidity distributions of produced particles normalized per one event. Top panel: normal baryons (solid line), all composite nucleon fragments (dashed line), and all composite hyper-fragments (thick dotted line). Bottom panel presents the same but for anti-particles. The UrQMD and CB calculations are performed for  $^{208}\text{Pb}$  on  $^{208}\text{Pb}$  collisions at  $\sqrt{s}=2.76$  A TeV overall impact parameters (minimal bias).

(cascade) version of UrQMD to generate baryons and their momenta. Then these are again used to form nuclei and hypernuclei via the CB model as described above. One should note here that the proton distributions fall more steeper with the transverse momentum than it was obtained in the hybrid version with hydrodynamics. Nevertheless, the main mechanisms of the particle production related to the secondary interactions remain the same, and the total particle and anti-particle yields are close. For this reason, the trends characterizing the modification of baryon momentum distributions with rapidity will be similar in the both

versions.

We demonstrate now predictions of the coalescent approach which are important for further investigations of the nuclear cluster formation in ultra-relativistic nuclear collisions. We have performed the UrQMD + CB calculations for all impact parameters with the minimum bias prescription. Fig. 3 shows the full rapidity distributions of baryons and obtained from them composite fragments of all sizes. For comparison, the top panel is for normal particles, and the bottom one is for anti-particles. Also we give separately fragments from nucleons and hyper-fragments which includes hyperons. We should note that in this and next figures we do not show the spectator nucleons and normal clusters composed from nucleons with rapidities around the projectile/target one (i.e., with  $|y| \approx 8$ ). Slow participant nucleons may exist in this region and form clusters within the coalescence model. However, the full consideration requires a detail description of the excitation and de-excitation (via particle emission) of spectator residues, that is beyond the present paper. Moreover, these clusters can hardly be measured in present experiments because of very high rapidities.

For clarity, we have demonstrated results for one coalescence parameter  $v_c = 0.1$ , which is reasonable for the description of the data (Fig. 1). One can see a very broad distribution of the produced baryons in the rapidity. At such a high energy nearly the same amount of normal and anti-baryons are present at central rapidities. The broad rapidity distribution of the yields have already been discussed at intermediate collision energies [17, 38]. It is seen from Fig. 3 that the production maximum for all composite fragments is shifted from midrapidity to the forward and backward region. In our case the wide maxima are located at the center-of-mass rapidities around +4 or -4. The reason of this phenomenon is in many secondary interactions and the energy loss during the hadron diffusion from midrapidity. An essential part of these interactions takes place between the newly produced species and the nucleons of projectile and target which did not interact in early times of the reaction. For this reason, both the energies and relative momenta of produced new baryons become smaller, therefore, it is easier for them to coalesce into a cluster. As a result of such processes the low-energy products mainly populate the phase space far from midrapidity. As another consequence of these secondary interactions we have found that the transverse momentum distributions of the produced particles decrease versus  $P_T$  more rapidly around  $|y| \approx 4$  than at  $|y| \approx 0$ .

Actually, the intensive interactions recall the thermalization process, therefore, under some conditions thermal models and phenomenologies may be applied to describe few characteristics of these reactions. In this respect, one can understand our results by assuming that the 'kinetic temperature' of baryons at midrapidity is much higher than this 'temperature' far from it. Therefore, the region outside midrapidity does contribute most strongly to the cluster production.

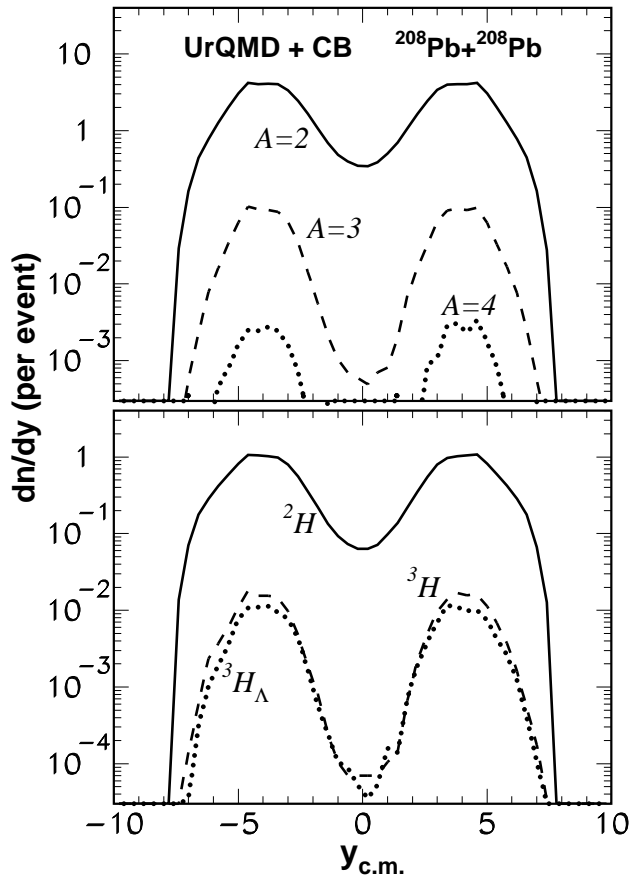


FIG. 4: The same as in Fig. 3, however, only for normal particles. Top panel: light clusters with sum baryon numbers  $A=2$ , 3, and 4 (solid, dashed and thick dotted lines respectively). Bottom panel presents rapidity distributions of individual particles: deuterons, tritons and hyper-tritons by solid, dashed and thick dotted lines respectively.

A more detailed picture of the light fragment production is given in Fig. 4. The top panel demonstrates the rapidity distributions of normal particle yields with mass (i.e., baryon)

numbers of  $A = 2$ ,  $A = 3$ , and  $A = 4$ . In this case all possible combinations of baryons (including both nucleons and hyperons) are taken into account, in order to understand the coalescence influence generally. One can see that the yield suppression of big fragments is much larger at midrapidity than in the region of the maximum fragment yield (at  $|y| \approx 4$ ). For this reason the exploration of heavy clusters is more promising at rapidities shifted from the midrapidity. This conclusion looks unexpected since more energy is deployed in central collisions at midrapidity. The reason is in the coalescence mechanism: The constituents should be not only produced, they should also have sufficiently low relative velocities to be bound into a cluster.

In the bottom panel of Fig. 4 we show the yields of selected particle clusters which can be easily identified in the experiment: deuterons ( ${}^2\text{H}$ ), tritons ( ${}^3\text{H}$ ), and hyper-tritons ( ${}^3_{\Lambda}\text{H}$ ), versus the rapidity. The distributions resemble the same structure as was discussed previously. One can clearly see from the figure that the yield ratio of  ${}^2\text{H}$  to  ${}^3\text{H}$  is around 800 at the midrapidity. Note that all calculations on this figure are performed for the coalescence parameters  $v_c = 0.1c$ , which slightly overestimates the deuteron production. Actually, this production and the corresponding ratio will be decreased by a factor of 2 when we take the more realistic  $v_c = 0.07c$ , as is clear from Fig. 1. However, one can see that even in the analysed case the deuteron-to-triton ratio is decreased to around 60 at  $|y| \approx 4$ . It is also naturally that the yields of  ${}^3\text{H}$  and  ${}^3_{\Lambda}\text{H}$  are very close, since at such high energy elementary hadron interactions new nucleons and hyperons are produced with similar probability.

The analysis tells us that the region in between the projectile/target rapidity and the center-of-mass rapidity is most favorable for the production of complex clusters consisting of newly produced baryons. We believe that experiments should take into account this phase space structure in searching for novel exotic nuclear species (including anti-nuclei). In relativistic heavy ion collisions besides the recently observed  ${}^3_{\Lambda}\text{H}$  nuclei [1, 3] other exotics (like  $\Lambda N$ ,  $\Lambda NN$ ) were under intensive discussions [6, 39]. The extension of measurements into a new rapidity region will increase the yields of clusters in the data substantially. It was shown in the LHCb experiments [40] that not only the midrapidity region but also particles with the rapidities around  $|y| \approx 4$  can be detected with the special detector set-up even at ultra-relativistic energies.

## V. CONCLUSION

It was demonstrated that the coalescence process is very important for the production of light baryonic clusters in ultrarelativistic nuclear collisions. We have shown that it is possible to describe spectra of the composite clusters measured by ALICE at LHC within our UrQMD + CB approach. We emphasized that the scaling of the elliptic flow of these particles may indicate the dominance of the coalescence mechanism.

The extension of the coalescence results beyond the central collisions demonstrate that the maximum yields of such clusters are not located at midrapidity. They are essentially shifted toward the target and projectile rapidities. This effect reflects the importance of the secondary interaction processes which lead to a considerable baryon production with low relative momenta. It may also be correlated with emerging the hadron fragmentation area. Such a new production phenomenon is especially important for forming large clusters. Yields of such clusters can be increased by many orders while going to the forward/backward region in comparison with the midrapidity zone. Here the formation of relatively big exotic, hyper- and anti-nuclei becomes very prominent and it is promising for future research, as it could provide a unique possibility to study novel nuclear species.

### Acknowledgments

A.S. Botvina acknowledges the support of BMBF (Germany). M. Bleicher thanks the COST Action THOR for support. The authors thank B. Dönigus for stimulating discussions.

- 
- [1] The STAR collaboration, *Science* **328**, 58 (2010).
  - [2] Y.-G. Ma (for STAR/RHIC collaboration), talk at NUFRA2013 conference, Kemer, Turkey, 2013, <http://fias.uni-frankfurt.de/historical/nufra2013/>.
  - [3] B. Dönigus *et al.* (ALICE collaboration), *Nucl. Phys. A* **904-905**, 547c (2013).
  - [4] P. Camerini (for ALICE/LHC collaboration), talk at NUFRA2013 conference, Kemer, Turkey, 2013, <http://fias.uni-frankfurt.de/historical/nufra2013/>.
  - [5] Y.G. Ma *et al.*, arXiv:1301.4902 (2013).
  - [6] B. Dönigus *for the ALICE collaboration*, *EPJ Web Conf.* **97**, 00013 (2015).

- [7] E.L. Bratkovskaya *et al.*, Phys. Rev. C **69**, 054907 (2004).
- [8] C. Hartnack *et al.*, Phys. Rep. **510**, 119 (2012).
- [9] S.A. Bass *et al.*, Prog. Part. Nucl. Phys. **41**, 225 (1998).
- [10] M. Bleicher *et al.*, J. Phys. G **25**, 1859 (1999).
- [11] A.S. Botvina *et al.*, Phys. Rev. C **95**, 014902 (2017).
- [12] J. Steinheimer and M. Bleicher, EPJ Web Conf. **97**, 00026 (2015).
- [13] J. Steinheimer, J. Aichelin, M. Bleicher and H. Stöcker, arXiv:1703.06638 [nucl-th].
- [14] V.D. Toneev, K.K. Gudima, Nucl. Phys. A**400** (1983) 173c.
- [15] M. Gyulassy, K. Frankel, E.A. Remler, Nucl. Phys. A**402** (1983) 596.
- [16] J.L. Nagle *et al.*, Phys. Rev. C**53** (1996) 367.
- [17] A.S. Botvina *et al.*, Phys. Lett. B **742**, 7 (2015).
- [18] A. Andronic, P. Braun-Munzinger, J. Stachel, H. Stöcker, Phys.Lett. B **697**, 203 (2011).
- [19] J. Steinheimer, K. Gudima, A. Botvina, I. Mishustin, M. Bleicher, H. Stöcker, Phys. Lett. B **714**, 85 (2012).
- [20] A. Andronic, P. Braun-Munzinger, K. Redlich, J. Stachel, Nucl. Phys. A **904-905**, 535c (2013).
- [21] J. Stachel, A. Andronic, P. Braun-Munzinger, K. Redlich, Journal of Phys.: Conf. Ser. **509**, 012019 (2014).
- [22] W. Neubert and A.S. Botvina, Eur. Phys. J. A **17**, 559 (2003).
- [23] H. Petersen, J. Steinheimer, G. Burau, M. Bleicher and H. Stöcker, Phys. Rev. C **78**, 044901 (2008).
- [24] J. Steinheimer, S. Schramm and H. Stöcker, Phys. Rev. C **84**, 045208 (2011).
- [25] F. Cooper and G. Frye, Phys. Rev. D **10**, 186 (1974).
- [26] F. Becattini, M. Bleicher, T. Kollegger, T. Schuster, J. Steinheimer and R. Stock, Phys. Rev. Lett. **111**, 082302 (2013).
- [27] F. Becattini, J. Steinheimer, R. Stock and M. Bleicher, Phys. Lett. B **764**, 241 (2017).
- [28] H.H. Gutbrod *et al.*, Phys. Rev. Lett. **37**, 667 (1976).
- [29] A.S. Botvina and J. Pochodzalla, Phys. Rev. C **76**, 024909 (2007).
- [30] A.S. Botvina, K.K. Gudima, J. Pochodzalla, Phys. Rev. C **88**, 054605 (2013).
- [31] J. Abelev *et al.* (ALICE collaboration), Phys. Rev. C **88**, 044910 (2013).
- [32] J. Adam *et al.* (ALICE collaboration), Phys. Rev. C **93**, 024917 (2016).
- [33] The ALICE collaboration, Journal of High Energy Physics **06**, 190 (2015).

- [34] X. Zhu, M. Bleicher, H. Stöcker, Phys. Rev. C **72**, 064911 (2005).
- [35] D. Molnar and S.A. Voloshin, Phys. Rev. Lett. **91**, 092301 (2003).
- [36] R. Anisbetty, P. Koehler and L. McLerrann, Phys. Rev. D **22**, 2793 (1980).
- [37] M. Li and J. I. Kapusta, arXiv:1702.00116 [nucl-th].
- [38] T. Anticic *et al.*, Phys. Rev. C **94**, 044906 (2016).
- [39] C. Rappold *et al.*, Phys. Rev. C **88**, 041001(R) (2013).
- [40] Y. Zhang *for LHCb collaboration*, arXiv:1605.07509 (2016).